

SUPPORTING INFORMATION

Reprogramming Cancer Cells by a BODIPY G-Quadruplex Stabiliser

Aminesena Baser, Beyza Basar, Hanim Beyza Dogan, Gulnur Sener, Nezahat Gokce Ozsamur, Fatma Secer Celik, Safaa Altves and Sundus Erbas-Cakmak*

Abstract:

A cationic BODIPY-based G-quadruplex-selective stabiliser is developed and shown to decrease cancer cell migration-invasion up to 90%. Expression of critical genes (HIF1 α , VIM, CDH1) related to the metastasis are modulated. Stabiliser reprograms hypoxia-adaptive metabolism and 1.82-fold increase in O₂ consumption, back-to-normal switching of energy metabolism is observed. Stabiliser with a strong G-quadruplex affinity (0.38 μ M K_d) significantly contributes to small molecule anti-cancer approach.

Table of Contents

Experimental Procedures	2
General Methods.....	2
Synthesis.....	2
FRET-Melting Analysis.....	3
UV-Vis Spectrophotometric Titration Analysis.....	3
Cell Viability Assay.....	3
Cell Migration and Invasion Assay.....	3
Oxygen Consumption Analysis	4
Gene Expression Analysis.....	4
Docking Analysis.....	5
Additional Figures.....	5
NMR and High-Resolution Mass Characterization Data.....	13
References.....	15

Experimental Procedures

General Methods

All chemicals, solvents, cell culture medium and ingredients were purchased from commercial companies and used without further purification unless otherwise indicated. Column chromatography for purifying the newly synthesized compounds was carried out using silica stationary phase (230–400 mesh, SiliCycle Inc., Canada). Analytical thin layer chromatography was performed on 0.25 mm thick precoated silica gel plates (60F254, Merck, Germany) and compounds were visualized using UV light. All ¹H NMR and ¹³C NMR spectra were recorded on a Varian Inova instrument (400 MHz) at Necmettin Erbakan University, Science and Technology Research and Application Center (BITAM). Chemical shifts (δ) are reported in parts per million (ppm) and referenced to the residual solvent peak. Coupling constants (J) are reported in hertz (Hz). Standard abbreviations indicating multiplicities are given b = broad, d = doublet, m = multiplet, s = singlet, t = triplet. High-resolution mass spectrometry was carried out using Agilent 6530 Accurate-Mass Q-TOF LC/MS (ESI) of the Eastern Anatolia Advanced Technology Research and Application Centre (DAYTAM, Erzurum, Turkey). For cell culture experiments MCF7 human breast adenocarcinoma cell line was used. Cells were visualized with Zeiss Inverted Microscopy. FRET-melting experiments and gene expression analysis were performed using Bio-rad CFX96 Real Time System qPCR instrument. Primers of PCR and G-quadruplex forming oligonucleotides labelled with FAM at 5' region and TAMRA dyes at 3' region as donor and acceptor probes respectively, were purchased from Sentebiolab, Ankara, Turkey. ImageJ software is used to quantify cell wound area. Statistical Analysis was done using GraphPad one-way ANOVA. Human umbilical vein endothelial cells (HUVEC) are kindly donated by Dr. Emine Nedime Korucu.

Synthesis

Compound **GQ1** was synthesized in 2 steps using the reactions shown in Scheme 1. Compound **1** were synthesized using previously described procedures reported in the literature.¹

Compound 2. In a round bottom flask 185 mg (0.42 mmol) and compound **1**, 4-pyridine carboxaldehyde (238 μl) were dissolved in 10 ml benzene. Piperidine (0.8 ml) and acetic acid (0.8 ml) were added. Dean-Stark apparatus was placed to the neck of flask and the mixture was refluxed for about 1 h until the reaction color turns into green. Product formation is monitored by thin layer chromatography (TLC) using acetone:hexane (1:1 volume/volume) as mobile phase. Reaction was allowed to cool R.T. Then extraction was done with water and dichloromethane. Organic phase was collected and dried with sodium sulfate. Solvent was evaporated under vacuo. The product was purified by silica column chromatography using the mobile phase mixture of acetone:EtOAc (1:1 volume/volume). Green solid was obtained with a yield of 5 %.

¹H NMR (400 MHz, CDCl₃) δ 8.57 (d, J = 6.1 Hz, 4H), 7.82 (d, J = 16.3 Hz, 2H), 7.40 (d, J = 6.3 Hz, 4H), 7.14 (d, J = 8.6 Hz, 2H), 7.08 (d, J = 16.3 Hz, 2H), 6.97 (d, J = 8.7 Hz, 2H), 6.61 (s, 2H), 4.00 (t, J = 6.0 Hz, 2H), 3.34 (t, J = 6.6 Hz, 2H), 1.95 – 1.83 (m, 2H), 1.83 – 1.71 (m, 2H), 1.46 (s, 6H).

¹³C NMR (101 MHz, CDCl₃) δ 159.74, 151.69, 150.33, 143.59, 143.27, 141.28, 134.50, 133.19, 129.37, 126.62, 123.26, 121.34, 118.48, 115.21, 67.38, 51.20, 26.52, 25.77, 14.96.

ESI-QTOF-MS: Theoretical m/z for (M + H)⁺: 616.2808; Experimental m/z for (M + H)⁺: 616.28205; Δ = 2.03 ppm.

Compound GQ1. 12 mg (0.02 mmol) compound **2** was dissolved in 2 ml dimethylformamide (DMF). 0.5 ml iodomethane was added and the mixture was stirred for 26 hours at RT. Then volatiles were evaporated under reduced vacuo. The solid product was washed with 1 ml ethyl acetate and 1 ml hexane solvent mixture, two times. Product was obtained as green solid in quantitative yield.

¹H NMR (400 MHz, DMSO-*d*₆) δ 8.92 (d, J = 7.0 Hz, 4H), 8.22 (d, J = 7.0 Hz, 4H), 7.95 (d, J = 16.3 Hz, 2H), 7.86 (d, J = 16.3 Hz, 2H), 7.39 (d, J = 8.7 Hz, 2H), 7.18 (d, J = 8.7 Hz, 2H), 4.33 (s, 6H), 4.11 (t, J = 6.2 Hz, 2H), 3.45 (t, J = 6.7 Hz, 2H), 1.92 – 1.79 (m, 2H), 1.78 – 1.68 (m, 2H), 1.55 (s, 6H).

ESI-QTOF-MS: Theoretical m/z for (M)²⁺: 322.65995; Experimental m/z for (M)²⁺: 322.65941; Δ = 1.67 ppm.

FRET-Melting Analysis

FRET Melting analysis with FAM and TAMRA labelled oligonucleotides were done using the previously described literature procedure.² HPLC-purified oligonucleotides are obtained commercially with FAM and TAMRA labels at 5' and 3' regions, respectively (Table S1). 0.2 μM oligonucleotides (*c-myc*, *bcl-2* and ds-DNA) in cacodylate buffer (10 mM sodium cacodylate, 0.1 M LiCl, at pH 7.2) was prepared with MiliQ purified water. FRET-melting analysis was done using 5 μM **GQ1** between the temperatures 25-95 °C by using qPCR (Bio-rad CFX96 C1000 Touch Real Time System). Following 5 min initial incubation at 25°C, the temperature was raised by 1 °C for every minute until it reaches 95 °C. Samples were excited at 492 nm and emission at 516 nm was followed as donor emission, as described in the literature.²

Table S1. Sequences of oligonucleotides used in FRET-melting assay² In FRET melting analysis oligonucleotides are labelled with 5' FAM and 3' TAMRA. For UV-Vis spectroscopic titration, oligomer with the same sequence, without any label, was used.

Oligomer	Sequence (5' to 3')
<i>c-myc</i>	TGG GGA GGG TGG GGA GGG TGG GGA AGG
<i>bcl-2</i>	AGG GGC GGG CGC GGG AGG AAG GGG GCG GGA GCG GGG CTG
<i>ds-DNA</i>	CAA AAA TTT TTG CAA AAA TTT TTG

UV-Vis Spectrophotometric Titration Analysis

Dissociation constant of **GQ1** for *c-myc* is estimated from UV-Vis absorption spectral change upon titration with unlabeled *c-myc* fragment. The sequence of the oligomer is given in Table S1, and this region mapped to -142 to -115 bp upstream of P1 promoter of this gene reported to form G-quadruplex.^{2e} 1 μM **GQ1** dissolved in cacodylate buffer (10 mM sodium cacodylate, 0.1 M LiCl, in MiliQ purified water, at pH 7.2) was titrated with small aliquots of *c-myc* oligomer. Change in the absorption at 650 nm was monitored and plotted. K_d (corresponding to 1/K_a) is calculated using the slope data of the Benesi-Hildebrand plot, using the formula below:

$$A_0/\Delta A = 1/(K_a \cdot \Delta A_0) [DNA] + 1/\Delta A_0 \quad \text{Equation 1}$$

where ΔA corresponds to absorbance change at 650 nm, A₀ is the initial absorbance value at the same wavelength.³

Cell Viability Assay

The human breast cancer cell line (MCF-7) or human umbilical vein endothelial cells (HUVEC) were used to study cellular toxicity. To determine **GQ1** cytotoxicity, cells were seeded on 96-well plate using HG-DMEM culture medium supplemented with 10% FBS and 0.2 % gentamicin and incubated at 37°C in 5% CO₂ in the incubator for 24 h (Thermo Scientific, Steri-cycle i160 CO₂ Incubator). Cells are either kept under normoxia or treated with 100 μM of CoCl₂·6H₂O to mimic hypoxia and incubated at 37°C in 5% CO₂ in the incubator for 24 h.⁴ Cobalt chloride is known to stabilize HIF1α protein as well as induce the expression of it therefore mimicking hypoxia environment. Then, different doses of **GQ1** were given to the medium at different doses (0-16 μM or 0-32 μM) and the cells are further incubated under the conditions given above for 24 more hours. Then, MTT was added and waited for 4 hours. Then 10 μl MTT solution (from the stock of 5 mg/ml) was added to each well containing 200 μl culture medium and mixed gently. After 4 h incubation in dark, resulting formazan crystals were dissolved in DMSO and absorbance at 570 nm was recorded. Data was used to calculate IC₅₀ value. The experiment was done with four replicates.

Cell Migration and Invasion Assays

MCF-7 cells were seeded on 24-well plate with a density of 5x10⁴ cells/well in 200 μL HG-DMEM culture medium supplemented with 10% FBS and 0.2 % gentamicin. The cells were incubated for 24 h at 37 °C in 5% CO₂ in the incubator. Cells are either kept under normoxia or treated with 100 μM of CoCl₂·6H₂O for 24 hours. **GQ1** stock solution was added to culture medium at 5 and 10 μM doses, either 1 hour or 24 hours before the formation of the scratch. In 24 h, cells form confluent monolayer and wounds are created with a pipette tip by scratching gently. Cell images were taken with an inverted light microscope for 48 h. For each group, change in area was normalized to initial wound area and then groups are compared to eliminate any discrepancies associated with initial wound shape. Wound areas were calculated with ImageJ software and statistical analyses were done by using GraphPad One-way ANOVA.

Invasion ability of cells was also analyzed using the cell invasion assay kit (ECM550, EMD Millipore Corp., USA). MCF-7 cells (1×10^5) were seeded and incubated for 24 hours at 37 °C. Four different experimental groups were analyzed: untreated hypoxic cells, treated hypoxic cells, untreated normoxic cells and treated normoxic cells. For hypoxic treated group, first cells are incubated under hypoxia for 24 hours prior to **GQ1** (10 μ M) addition. Cells are further incubated for 24 hours. Cells were then lifted and added to the porous wells with serum-free medium. HG-DMEM was added to the bottom of the porous well. After 16 hours, the medium was removed from the porous well and washed twice with PBS. 4% paraformaldehyde was added to fix the cells for 2 min at RT then 4% paraformaldehyde was discarded and washed twice with PBS. 100% methanol was added and kept at -20 for 20 minutes. Then methanol was discarded and washed twice with PBS. Giemsa stain was added and incubated at RT for 15 minutes. Then Giemsa was discarded and washed twice with PBS. The non-migrating cells located above porous well were removed with a cotton swab. Migrating cells were visualized and counted under an inverted light microscope. Statistical analyses were made using GraphPad One-way ANOVA.

Oxygen Consumption Analysis

MCF-7 cells were seeded on flat, black bottom 96-well plate with a density of 10×10^5 cells/well in 200 μ L HG-DMEM culture medium supplemented with 10% FBS and 0.2 % gentamicin. The cells were incubated for 24 h at 37 °C in 5% CO₂ in the incubator. Cells are either kept under normoxia or treated with 100 μ M of CoCl₂.6H₂O to mimic hypoxia and incubated under the same conditions for 24 hours. After 24 h incubation, cells were treated with **GQ1** (5 μ M or 10 μ M) and incubated for a further 24 h at 37 °C in 5% CO₂ incubator. Oxygen consumption was measured by Oxygen Consumption Rate Assay Kit (Cayman Chemical Item no: 600800) using the recommended procedure. Following the probe addition, fluorescence measurement was taken with the absorbance microplate reader (Agilent BioTek Epoch Microplate Spectrophotometer) by setting the excitation wavelength to 380 nm and following the emission at 650 nm. The experiment was done with three replicated and statistical analysis was performed using GraphPad software.

Gene Expression Analysis

MCF-7 cells were incubated with a cell density of 5×10^6 cells/well either under normoxic or hypoxic conditions for 24 h using the medium and incubation conditions given above. Hypoxic conditions are generated by adding CoCl₂.6H₂O into the culture medium, with a final concentration of 100 μ M, as described above. **GQ1** (10 μ M) was added to the culture medium and then incubated under normoxic or hypoxic conditions for an additional 24 h. Then, GeneJET RNA purification kit (Thermo Scientific, GeneJet, K0731) was used for RNA isolation. NanoDrop (Epoch 2 Microplate Reader) was used to quantify and check the purity of RNA samples. PrimeScript 1st strand cDNA synthesis kit (Takara: 6110A-50) was used for cDNA synthesis. RT-qPCR analysis was done using the primers for the genes given in Table S2, by using SYBR Green Supermix (Bio-Rad) using Bio-Rad CFX Connect. For RT-qPCR, the following procedure is used: initial denaturation at 95°C for 30 seconds, denaturation at 95°C for 15 seconds, annealing at 60°C for 30 seconds, and extension at 72°C for 30 seconds. Annealing and extension steps were performed for 39 cycles. Experiments were repeated at least three times. The RT-qPCR analysis was performed using β -actin under normoxia as internal control by using the $2^{-\Delta\Delta Ct}$ method. Statistical Analysis was done using GraphPad one-way ANOVA.

To prove that **GQ1** has no effect on genes lacking G-quadruplex in their promoters, reference gene expression level is also analysed. TATA-binding protein, *tbp* is reported to lack putative G-quadruplex structures neither in its promoter nor in mRNA.⁵ No significant change is observed in the expression of this gene after treatment with **GQ1** suggesting the selective activity of the ligand on G-quadruplex bearing genes (Figure S7).

Table S2. Sequences of primers used in RT-PCR

Gene	Forward Sequence (5' to 3')	Reverse Sequence (5' to 3')
VIM	AGGCAAAGCAGGAGTCCACTGA	ATCTGGCGTTCCAGGGACTCAT
MMP7	CCTCCACTCACTATGTAGA	ATTCTTATCTCCAACCTTCCAA
WNT1	CTGTCCTGCCTCCTCATC	GGACCCAGCACATAAATAGTT
ZEB2	TTTGCCCAACTGCTGACC	GCTACAGAGAGGGCAGGAA
CDH1	GCC TCC TGA AAA GAG AGT GGA AG-3' -23 bp	TGG CAG TGT CTC TCC AAA TCC G
GLUT1	GCTACAACACTGGAGTCATCAA	ACTGAGAGGGACCAGAGC
COX4-II	GAAGACGAGGGATGCACAG	GGCTCTTCTGGCATGGG
PDK1	CATGTCACGCTGGGTAATGAGG	CTCAACACGAGGTCTTGGTGCA
HIF1 α	TAT GAG CCA GAA GAA CTT TTA GGC	CAC CTC TTT TGG CAA GCA TCC TG
ACTB	CAC CAT TGG CAA TGA GCG GTTC	AGG TCT TTG CGG ATG TCC ACG T
TBP	TGTATCCACAGTGAATCTTGTTG	GGTTCGTGGCTCTCTTATCCTC

Docking Analysis

To predict the G4 binding mode of **GQ1**, molecular docking studies are performed using AutoDock 4.2 software.⁶ Ligand conformation was searched using the Lamarckian algorithm. Binding is analysed using MYC G-quadruplex experimental structure (accession number 7kbx), obtained from the RCSB protein databank and used after removing the bound ligand from the structure.^{6b} Analysis is performed by setting the Grid Box to cover the entire G-quadruplex structure. 2Å root-mean-square cluster tolerance is used, mutation rate is 0.02. 100 docking trials are performed. Boron of the **GQ1** ligand compound is replaced with carbon to facilitate the analysis as also suggested in literature.^{6c} Results of van der Waals (vdW) interactions, desolvation energies (desolv), Hydrogen bonding (Hbond) energies are given in kcal/mol units.

Additional Figures

Binding constant for G-quadruplex DNA was determined using UV-Vis titration and Benesi-Hildebrand equation.^[16] The dissociation constant is determined to be 0.38 μM (Figure S1).

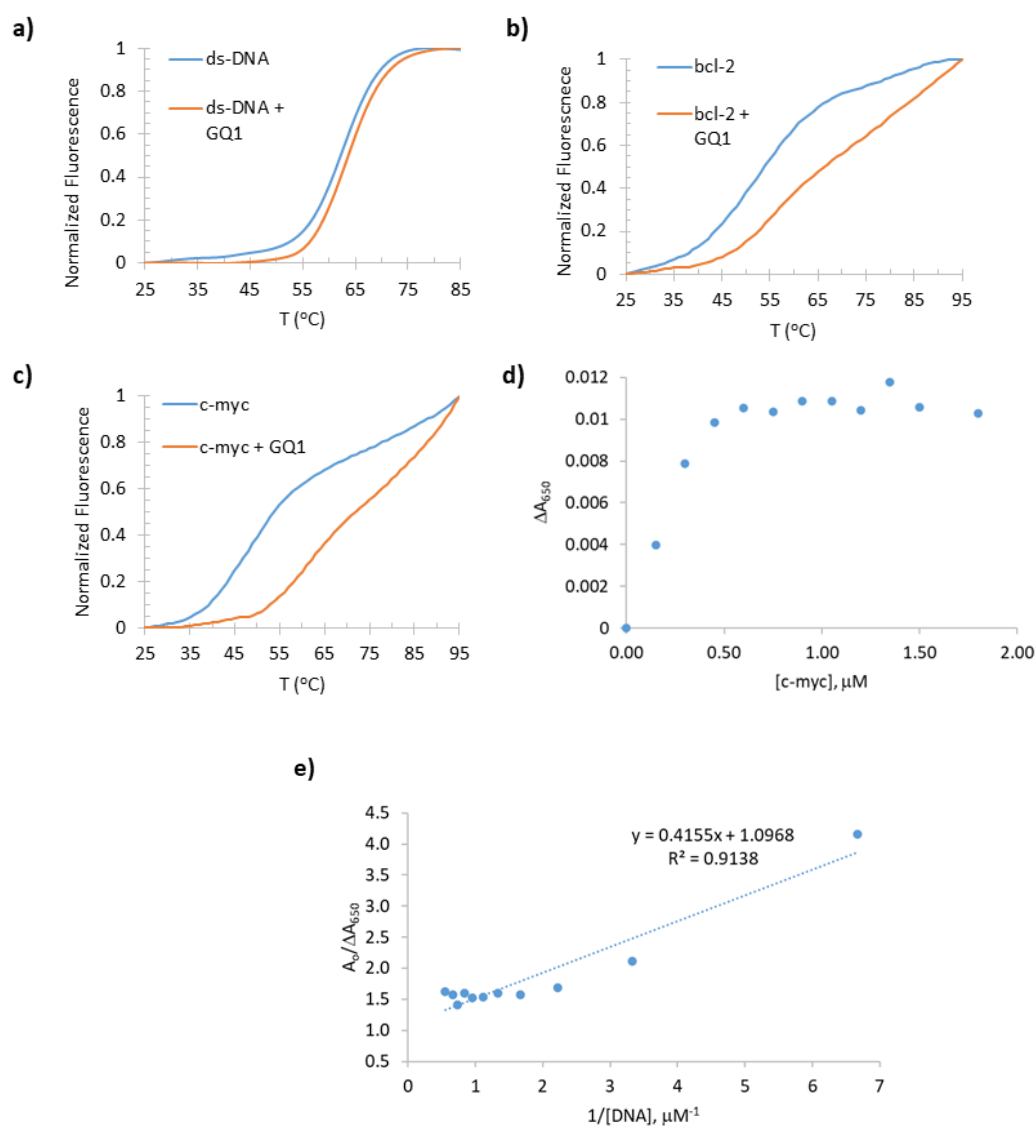


Figure S1. FRET-Melting analysis of GQ1 (a-c). Oligomers (ds-DNA, c-myc, bcl-2, each 0.2 μM) were used with/without 5 μM GQ1 (n=3). (d) Titration of GQ1 (1 μM) with unlabelled c-myc oligomer followed by UV-Vis absorbance at 650 nm. Experiments were run in sodium cacodylate buffer at pH 7. Benesi Hildebrand plot of **GQ1** titrated with c-myc oligomer (e).

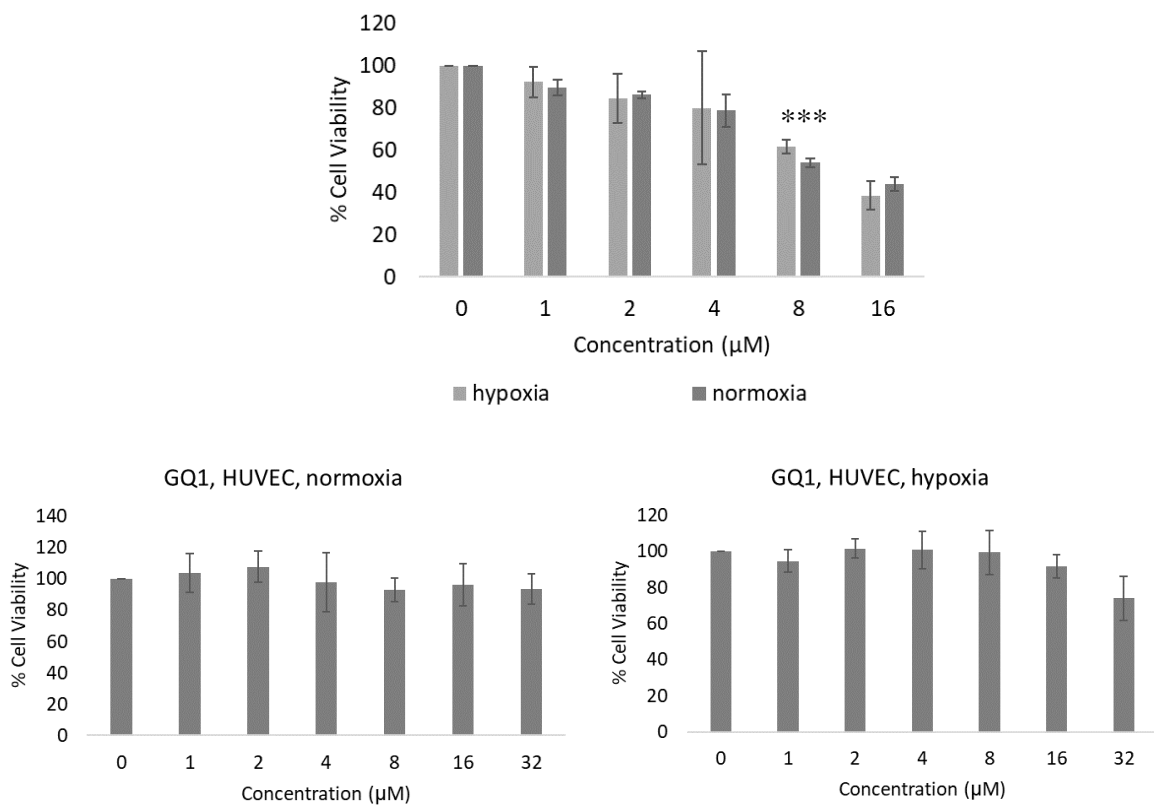


Figure S2. Cytotoxicity of **GQ1** to MCF7 cancer and HUVEC healthy cells under normoxia and hypoxia. Hypoxia was generated with $\text{CoCl}_2 \cdot 6\text{H}_2\text{O}$ (100 μM). (n = 4, ***p < 0.001). At application dose, 10 μM or below, **GQ1** is not toxic to healthy cells.

From the graphs shown in Figures S2, S3 and S4, IC_{50} value of **GQ1** under normoxia and hypoxia was calculated to be 12.48 μM and 12.20 μM respectively. **GQ1** is not toxic to HUVEC healthy human cells at application concentrations.

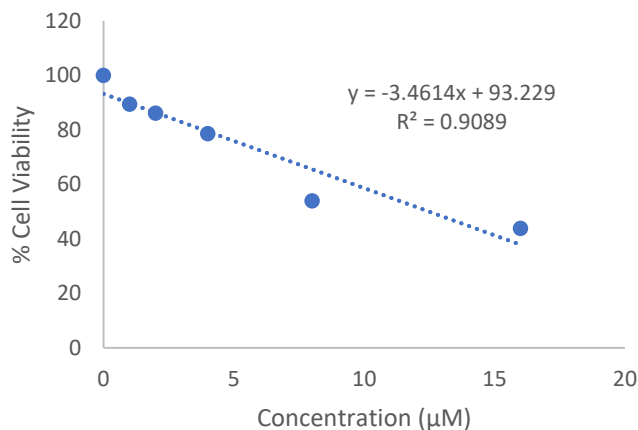


Figure S3. Percent viability of MCF7 cells in the presence of different concentrations of **GQ1** under normoxia.

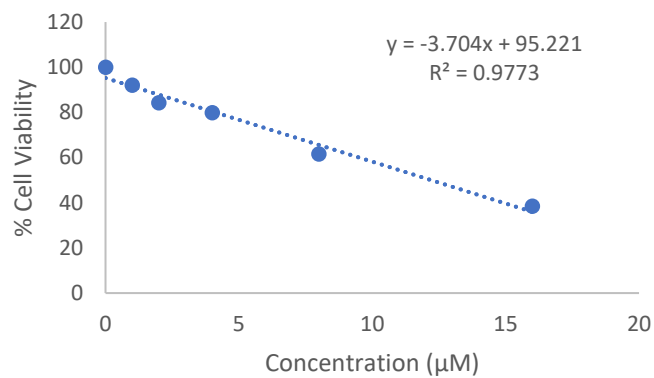


Figure S4. Percent viability of MCF7 cells in the presence of different concentrations of **GQ1** under hypoxia.

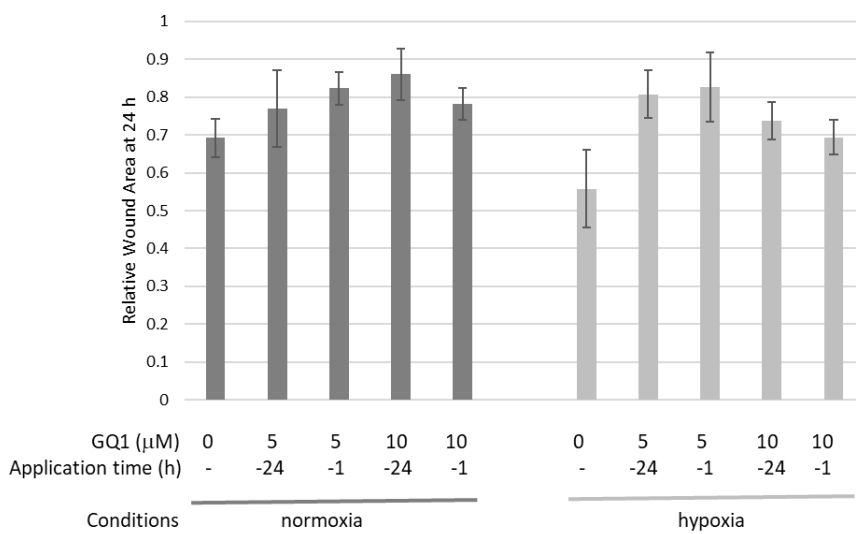


Figure S5. Change in the wound area when cells are exposed to normoxic and hypoxic conditions in the presence or absence of **GQ1** (5 or 10 µM). **GQ1** is introduced to cell medium at either 1 or 24 h prior to wound generation. Relative wound area is calculated by normalizing the data at 24 h with respect to initial cell control group. (n = 3)

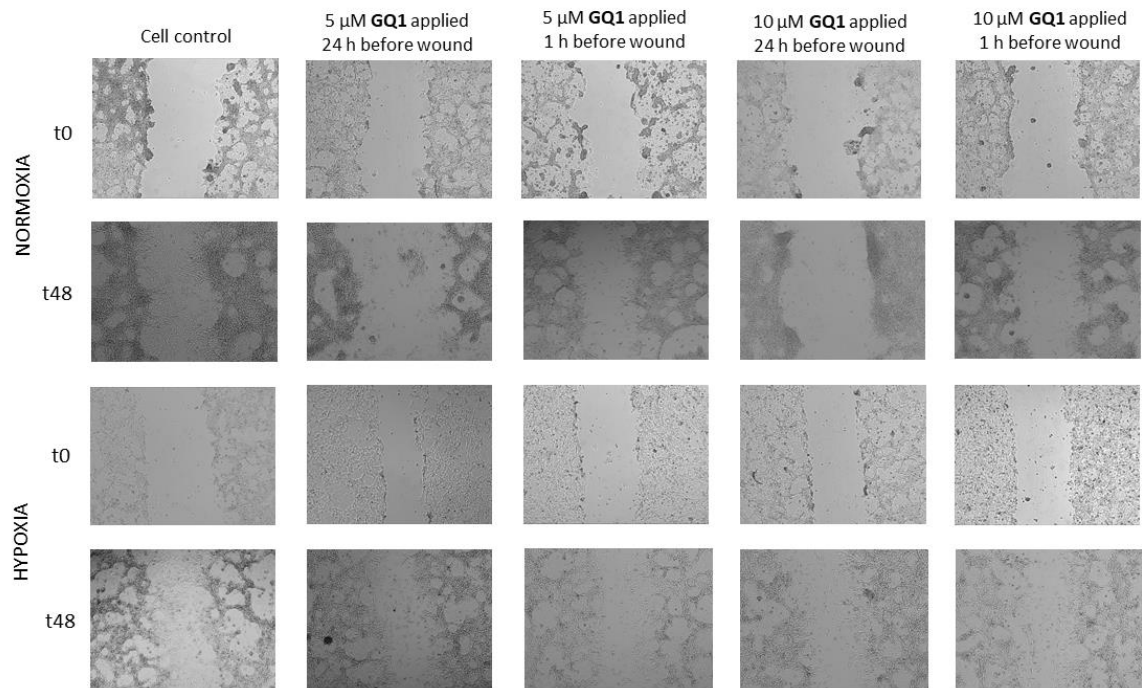


Figure S6. Microscope images of cells under normoxic and hypoxic conditions in the presence or absence of **GQ1** (5 or 10 μM). **GQ1** is introduced to cell medium at either 1 or 24 h prior to wound generation. Representative photos are taken immediately after wound formation and 48 h after wound generation.

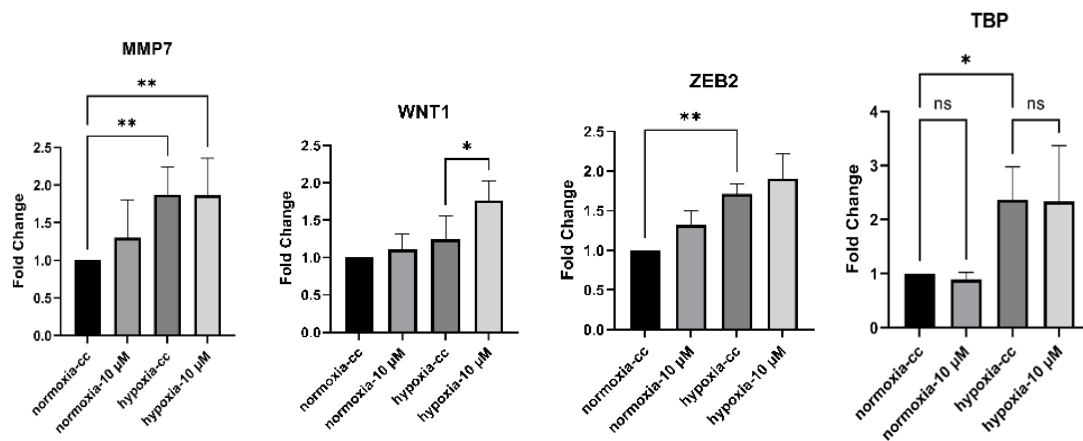


Figure S7. Fold change in mRNA expression of MCF7 cells in the presence of **GQ1** (10 μM) under hypoxia and normoxia. β -actin is used as internal control. ($n \geq 3$, $*p < 0.05$; $**p < 0.005$). Expression of TBP, which is reported to have no putative G-quadruplex in the promoter region is also analysed as negative control group.⁵ **GQ1** has no effect on the expression of this gene, neither under hypoxia nor under normoxia suggesting that GQ1 selective modulates G-quadruplex bearing genes or the genes found in the downstream pathway.

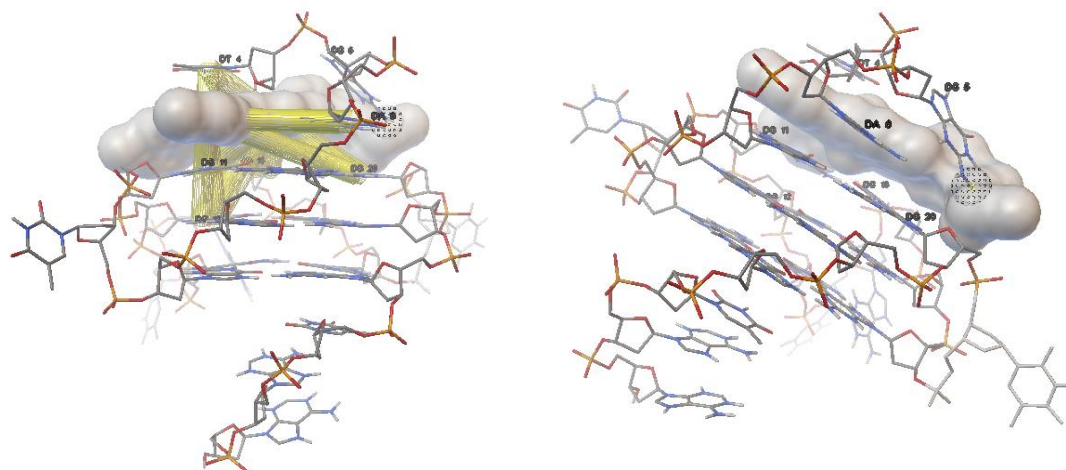


Figure S8. Interaction of **GQ1** with c-myc G-quadruplex structure, as predicted by AutoDock 4.2 software.

Docking analysis using AutoDock software predicted $-9.2 \text{ kcal. mol}^{-1}$ binding energy and $179.27 \text{ nM}^{-1} K_d$ value. π - π interaction between guanine of G4 plane and the BODIPY main conjugated body (left figure, bottom yellow interactions) is observed. Additional π - π interaction between thymine base and the pyridine residue is observed (left figure, top yellow interaction). One Hydrogen bond is predicted between guanine NH_2 and azide moiety (right figure, interaction shown with a sphere). Pyridinium cations are lying towards phosphate groups and electrostatic energy contribution is estimated to be $-0.22 \text{ kcal.mol}^{-1}$. Summary of energy contributions are listed below:

Estimated Free Energy of Binding = -9.20 kcal/mol [= (1)+(2)+(3)-(4)] [Temperature = 298.15 K]

(1) Final Intermolecular Energy = -12.49 kcal/mol

vdW + Hbond + desolv Energy = -12.27 kcal/mol

Electrostatic Energy = -0.22 kcal/mol

(2) Final Total Internal Energy = -2.07 kcal/mol

(3) Torsional Free Energy = $+3.28 \text{ kcal/mol}$

(4) Unbound System's Energy [= (2)] = -2.07 kcal/mol

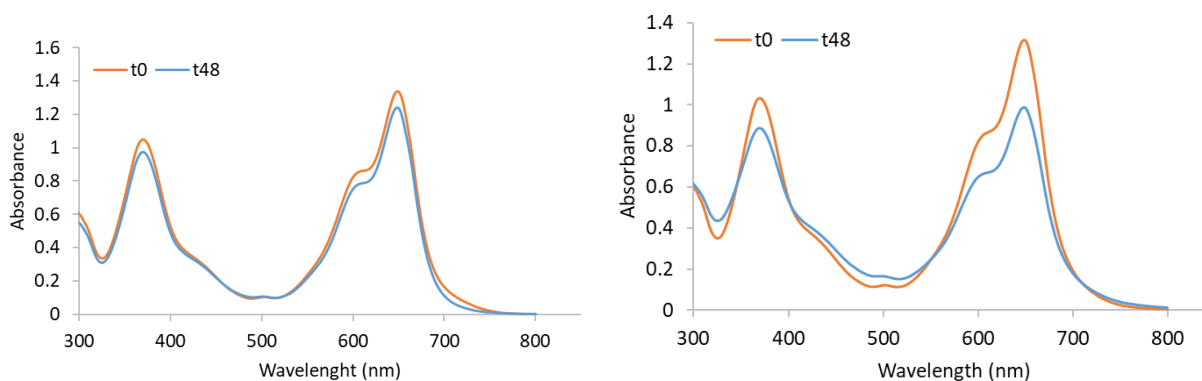


Figure S9. To investigate the stability of the **GQ1**, compound ($100 \mu\text{M}$) is dissolved in either PBS or culture medium HG-DMEM. Absorbance of the compound is measured initially and after 48 h incubation at 37°C . There is not a significant change in the peak shape in both solvents indicating the core stability of the compound under experimental conditions. A small decrease in the absorption of the compound in DMEM medium is attributed to partial aggregation after 2 days of incubation.

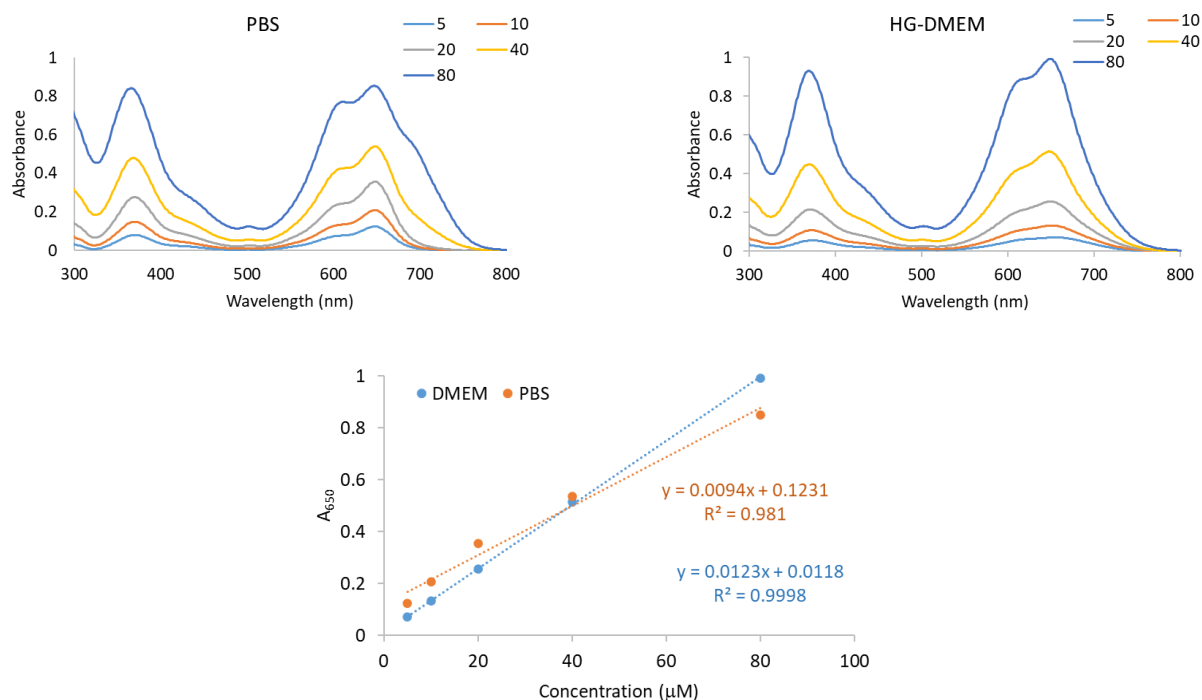


Figure S10. UV-Vis absorbance spectra of GQ1, (5-80 μM) in PBS or in HG-DMEM. is dissolved in either PBS or culture medium HG-DMEM. Linear dependency of the concentration on peak absorbance value at 650 nm (bottom figure) indicates that the compound is soluble in both solvents at the 5-80 μM concentration range at room temperature. Spectra of the compound at room temperature is slightly broader than the sample at 37°C (Figure S9) which may indicate better solubility at incubation temperatures.

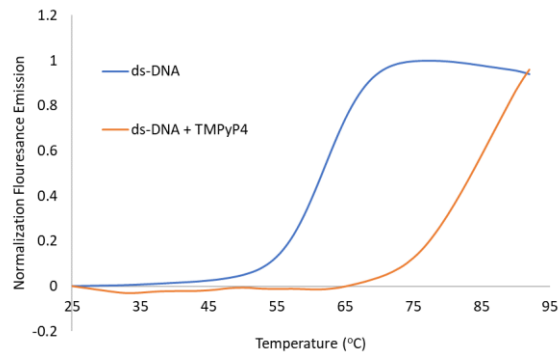


Figure S11. FRET-Melting analysis of commercial TMPyP4. Oligomer (ds-DNA, 0.2 μM) is used with/without 5 μM TMPyP4 (n=3). Compound significantly change the melting temperature of random DNA.

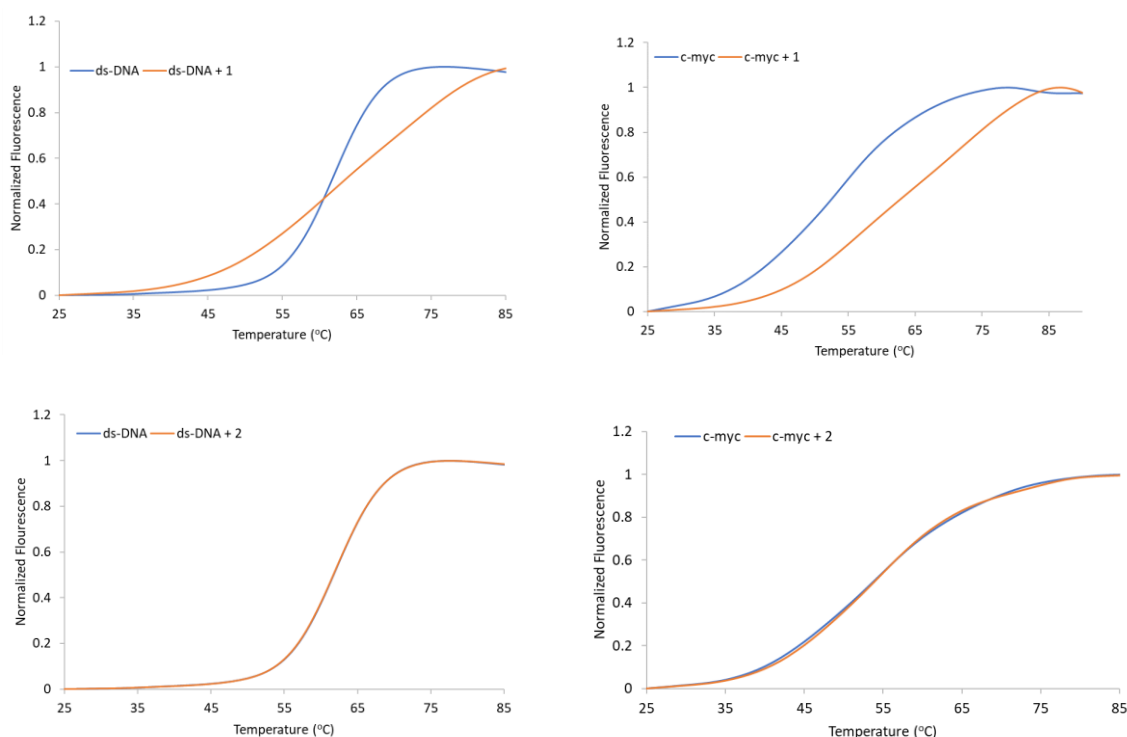


Figure S11. FRET-Melting analysis of compounds 1 and 2. Oligomer (ds-DNA, 0.2 μ M) is used with/without 5 μ M TMPyP4 (n=3). Compound 2 display no change in T_m values whereas compound 1 results in a shift of 1 and 10 10°C for ds-DNA and c-myc respectively. Compound 1 itself has absorbance at 521 nm which might interfere with FAM emission.

To compare the cellular effect of **GQ1** to commercially available G-quadruplex stabilizer, TMPyP4, MCF7 cells and HUVEC healthy human cells are exposed to the compounds and viabilities are analysed using the MTT procedure described above (Figure S12).⁷ As negative control group compound **2** is also tested, since this compound does not bind to G-quadruplex (Figure S11). None of the compounds are toxic to HUVEC cells below 32 μ M. This result shows that **GQ1** is safe for healthy cell HUVEC. TMPyP4 and compound **2** are also less toxic than **GQ1** to MCF7 cancer cells at the same concentration range suggesting a better therapeutic potential of **GQ1** in selected cancer cell model. Low selectivity of the TMPyP4 to G-quadruplex structures (Figure S11) compared to **GQ1** (Figure S1) also points the improved properties of the BODIPY based **GQ1** ligand. At low doses (as low as 0.25 μ M) TMPyP4 is reported to induce cell migration, which is not apparently wanted for cancer cells.⁸

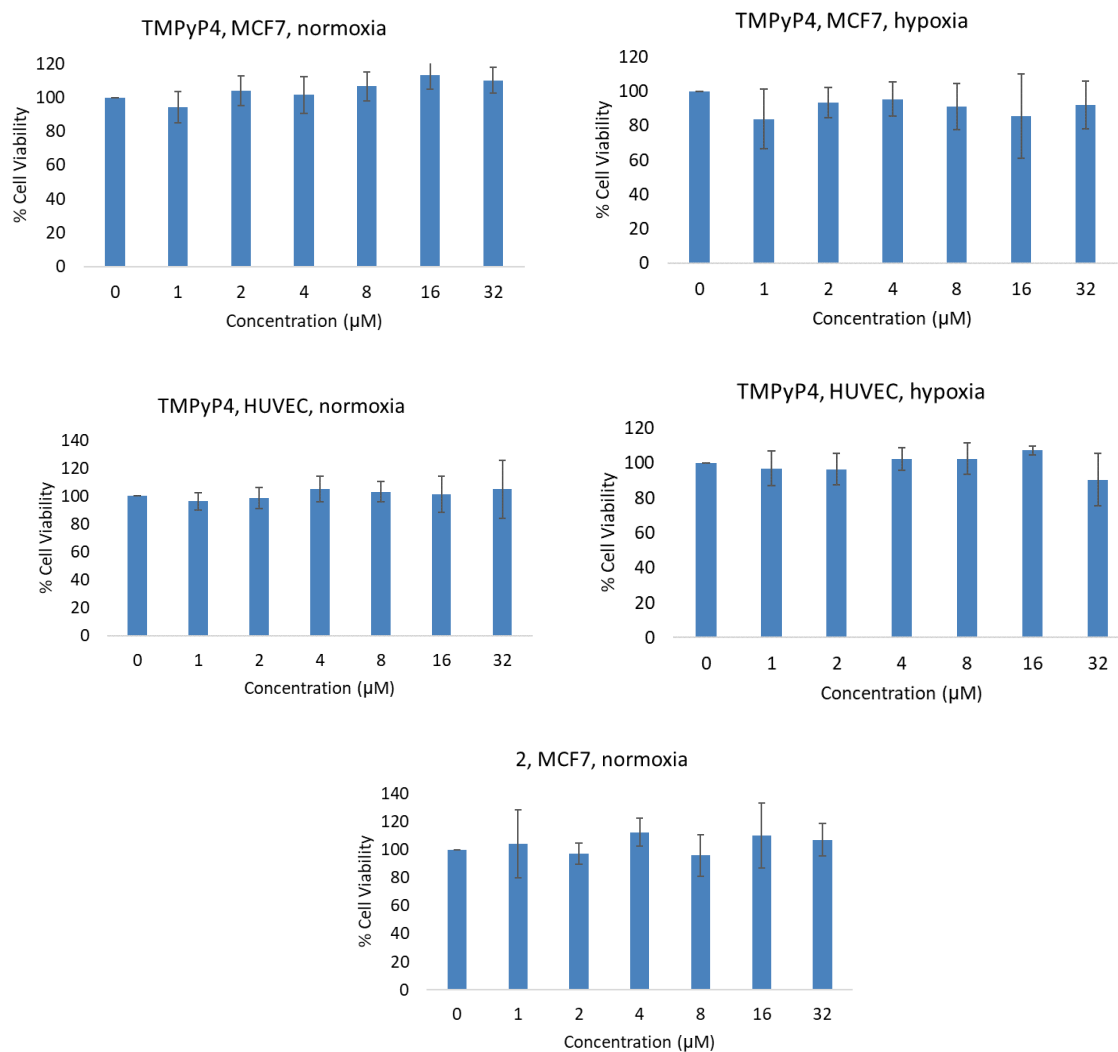


Figure S12. Cytotoxicity of compound **2** and TMPyP4 to MCF7 cancer and HUVEC healthy cells under normoxia and hypoxia. Hypoxia was generated with $\text{CoCl}_2 \cdot 6\text{H}_2\text{O}$ (100 µM). (n = 4). TMPyP4 is not toxic to MCF7 consistent with literature.⁹

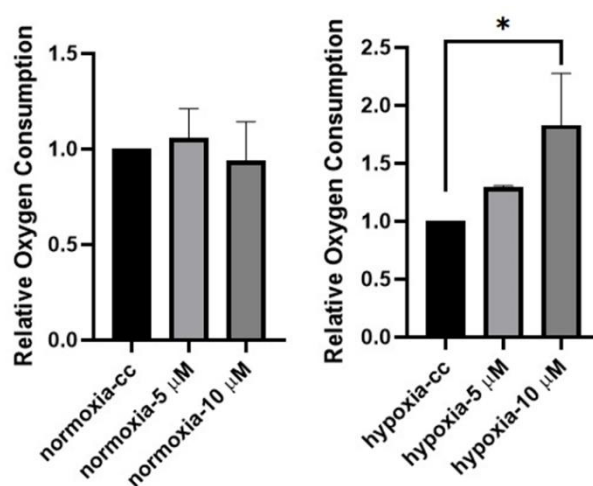
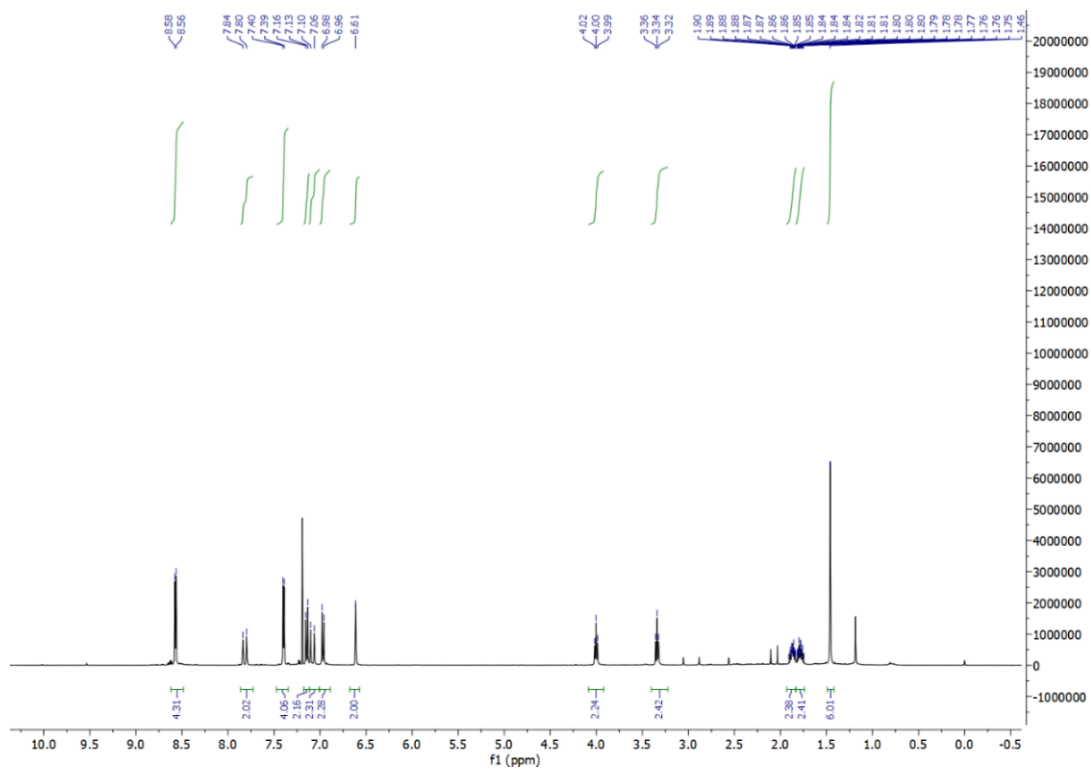
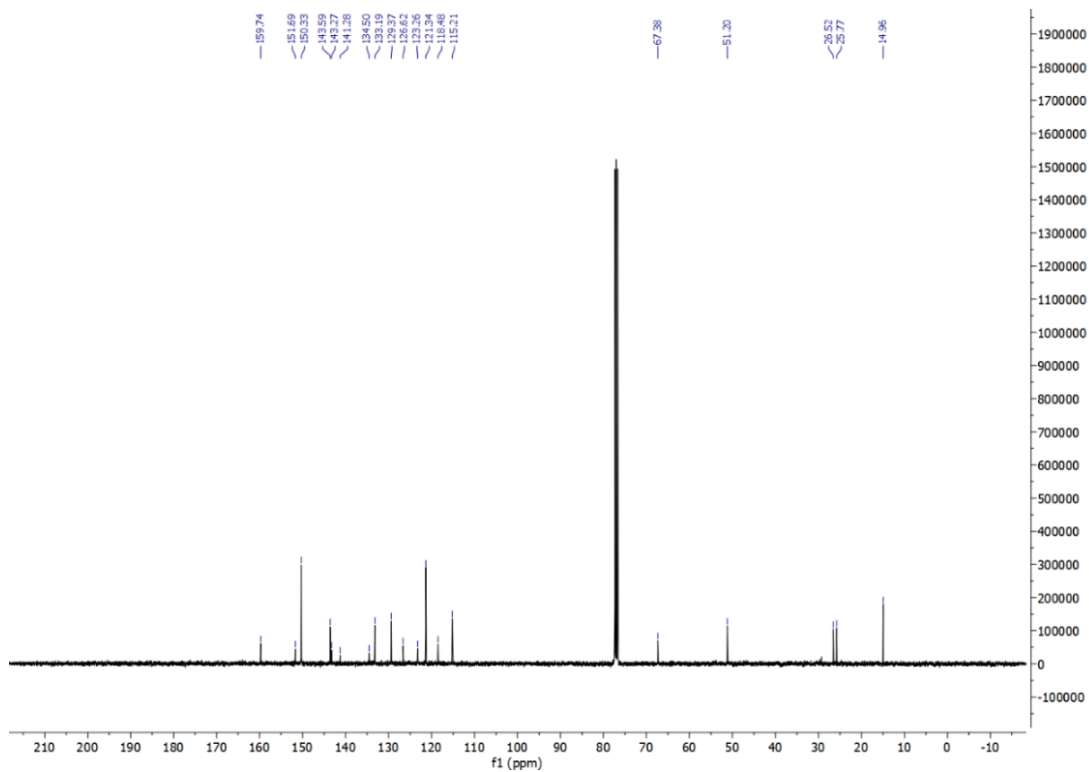


Figure S13. Relative oxygen consumption of MCF7 cells in the presence/absence of **GQ1** (5 or 10 µM). Cells are treated with **GQ1** for 24h and O_2 probe is added. Emission at 650 nm was recorded 125 minutes after the probe addition (λ_{exc} is 380 nm, n = 3, * p=0.0135)

NMR and High-Resolution Mass Characterization Data

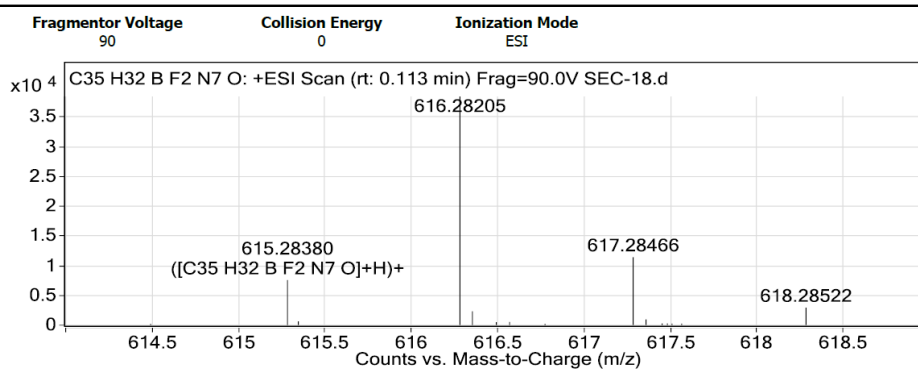


FigureS8. ¹H NMR spectrum of compound 2 (400 MHz, CDCl₃).

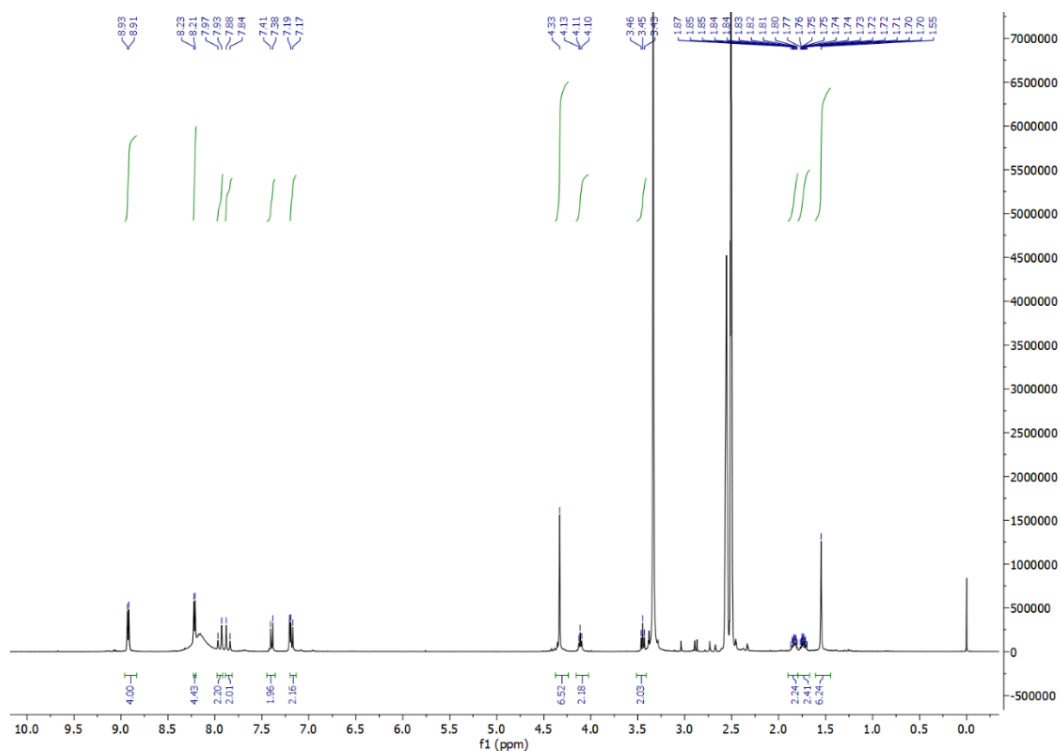


FigureS9. ¹³C NMR spectrum of compound 2 (101 MHz, CDCl₃).

User Spectra

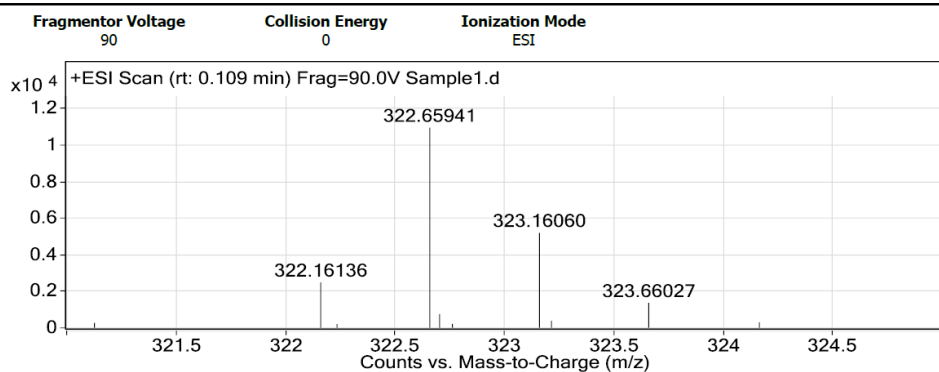


FigureS10. High-Resolution ESI-MS spectrum of compound 2.



FigureS11. ^1H NMR spectrum of compound GQ1 (400 MHz, d -DMSO).

User Spectra



FigureS12. High-Resolution ESI-MS spectrum of compound GQ1.

References:

- 1 G. Turkoglu, G. Kayadibi Koygun, M. N. Z. Yurt, S. Pirencioglu, S. Erbas-Cakmak, *Chem. Sci.* 2021, **12**, 9754.
- 2 (a) E. P. Lombardi, A. Holmes, D. Verga, M.P. Teulade-Fichou, A. Nicolas, A. Londoño-Vallejo, *Nucleic Acid Res.* 2019, **47**, 6098; (b) M. di Antonio, A. Ponjavic, A. Radzevičius, R. T. Ranasinghe, M. Catalano, X. Zhang, J. Shen, L.M. Needham, S. F. Lee, D. Klenerman, S. Balasubramanian, *Nat. Chem.* 2020, **12**, 832; (c) A. Fekete, E. Kenesi, E. Hunyadi-Gulyas, H. Durgo, B. Berko, Z. A. Dunai, P. I. Bauer, *Plos One*, 2012, **7**, e42690; (d) A. Terenzi, D. Lötsch, S. van Schoonhoven, A. Roller, C. R. Kowol, W. Berger, B. K. Keppler, G. Barone, *Dalton Trans.* 2016, **45**, 7758; (e) D. Yang, L. H. Hurley, *Nucleos. Nucleot. Nucl.* 2006, **25**, 951.
- 3 (a) H.A. Benesi, J.H. Hildebrand, *J. Am. Chem. Soc.* 1949, **71**, 2703; (b) R.M. Uda, N. Nishimoto, T. Matsui, S. Takagi, *Soft Matter*, 2019, **15**, 4454.
- 4 (a) M. Kaczmarek, R. E. Cachau, I. A. Topol, K. S. Kasprzak, A. Ghio, K. Salnikow, *Toxicol. Sci.* 2009, **107**(2), 394; (b) J. Muñoz-Sánchez, M. E. Chánez-Cárdenas, *J. Appl. Toxicol.* 2019, **39**(4), 556; (c) Y. Yuan, G. Hilliard, T. Ferguson, D. E. Millhorn, *J. Biol. Chem.* 2003, **278**, 15911; (d) N. K. Rana, P. Singh, B. Koch, *Biol. Res.* 2019, **2**, Article No: 12.
- 5 (a) J. F. Moruno-Manchon, E.C. Koellhoffer, J. Gopakumar, S. Hambarde, N. Kim, L. D. McCullough, A. S. Tsvetkov, *Aging*, 2017, **9**, 1957; A. A. Surani, C. Montiel-Duarte, *STAR Protoc.* 2022, **3**(2), 101372.
- 6 (a) G. M. Morris, R. Huey, W. Lindstrom, M. F. Sanner, R. K. Belew, D. S. Goodsell, A. J. Olson, 2009, *J. Comput. Chem.* 2009, **16**, 2785; (b) J. Dickerhoff, J. Dai, D. Yang, *Nucleic Acids Res.*, 2021, **49**, 5905; (c) R. Tiwari, K. Mahasenan, R. Pavlovicz, C. Li, W. Tjarks, *J. Chem. Inf. Model*, 2009, **49**, 1581; (d) Scripps Research, 2014. AutoDock, Available at: <https://ccsb.scripps.edu/autodock/>.
- 7 E. Izbicka, R. T. Wheelhouse, E. Raymond, K. K. Davidson, R. A. Lawrence, D. Sun, B. E. Windle, L. H. Hurley, D. D. Von Hoff, *Cancer Res.* 1999, **59**(3), 639.
- 8 X.-H. Zheng, X. Nie, H.-Y. Liu, Y.-M. Fang, Y. Zhao, L.-X. Xia, *Sci. Rep.* 2016, **6**, 26592.
- 9 N. Konieczna, A. Romaniuk-Drapała, N. Lisiak, E. Totoń, A. Paszel-Jaworska, M. Kaczmarek, B. Rubiś, *Int. J. Mol. Sci.* 2019, **20**(11), 2670.